American Journal of Ophthalmology Case Reports 7 (2017) 14–19

Contents lists available at ScienceDirect

American Journal of Ophthalmology Case Reports

journal homepage: http://www.ajocasereports.com/

Brief reports

Dysflective cones: Visual function and cone reflectivity in long-term follow-up of acute bilateral foveolitis

Joanna H. Tu [a, b], Katharina G. Foote [c], Brandon J. Lujan [c, d], Kavitha Ratnam [c], Jia Qin [a], Michael B. Gorin [e], Emmett T. Cunningham Jr. [d, f, g, h], William S. Tuten [c], Jacque L. Duncan [a, *], Austin Roorda [c]

[a] Department of Ophthalmology, 10 Koret Way, University of California San Francisco, San Francisco, CA, USA
[b] College of Physicians and Surgeons, Columbia University, New York, NY, USA
[c] School of Optometry and Vision Science Graduate Group, University of California Berkeley, Berkeley, CA, USA
[d] West Coast Retina Medical Group, San Francisco, CA, USA
[e] Stein Eye Institute, Department of Ophthalmology, University of California Los Angeles, Los Angeles, CA, USA
[f] Department of Ophthalmology, California Pacific Medical Center, San Francisco, CA, USA
[g] Department of Ophthalmology, Stanford University School of Medicine, Stanford, CA, USA
[h] The Francis I. Proctor Foundation, University of California San Francisco, School of Medicine, San Francisco, CA, USA

ARTICLE INFO

Article history:
Received 5 September 2016
Received in revised form
26 January 2017
Accepted 10 April 2017
Available online 12 April 2017

Keywords:
Optical coherence tomography
Adaptive optics scanning laser ophthalmoscopy
Multimodal imaging
Functional testing
Microperimetry

ABSTRACT

Purpose: Confocal adaptive optics scanning laser ophthalmoscope (AOSLO) images provide a sensitive measure of cone structure. However, the relationship between structural findings of diminished cone reflectivity and visual function is unclear. We used fundus-referenced testing to evaluate visual function in regions of apparent cone loss identified using confocal AOSLO images.

Methods: A patient diagnosed with acute bilateral foveolitis had spectral-domain optical coherence tomography (SD-OCT) (Spectralis HRA + OCT system [Heidelberg Engineering, Vista, CA, USA]) images indicating focal loss of the inner segment-outer segment junction band with an intact, but hyperreflective, external limiting membrane. Five years after symptom onset, visual acuity had improved from 20/80 to 20/25, but the retinal appearance remained unchanged compared to 3 months after symptoms began. We performed structural assessments using SD-OCT, directional OCT (non-standard use of a prototype on loan from Carl Zeiss Meditec) and AOSLO (custom-built system). We also administered fundus-referenced functional tests in the region of apparent cone loss, including analysis of preferred retinal locus (PRL), AOSLO acuity, and microperimetry with tracking SLO (TSLO) (prototype system). To determine AOSLO-corrected visual acuity, the scanning laser was modulated with a tumbling E consistent with 20/30 visual acuity. Visual sensitivity was assessed in and around the lesion using TSLO microperimetry. Complete eye examination, including standard measures of best-corrected visual acuity, visual field tests, color fundus photos, and fundus auto-fluorescence were also performed.

Results: Despite a lack of visible cone profiles in the foveal lesion, fundus-referenced vision testing demonstrated visual function within the lesion consistent with cone function. The PRL was within the lesion of apparent cone loss at the fovea. AOSLO visual acuity tests were abnormal, but measurable: for trials in which the stimulus remained completely within the lesion, the subject got 48% correct, compared to 78% correct when the stimulus was outside the lesion. TSLO microperimetry revealed reduced, but detectible, sensitivity thresholds within the lesion.

Conclusions and importance: Fundus-referenced visual testing proved useful to identify functional cones despite apparent photoreceptor loss identified using AOSLO and SD-OCT. While AOSLO and SD-OCT appear to be sensitive for the detection of abnormal or absent photoreceptors, changes in photoreceptors that are identified with these imaging tools do not correlate completely with visual function in every patient. Fundus-referenced vision testing is a useful tool to indicate the presence of cones that may be

* Corresponding author. Department of Ophthalmology, University of California San Francisco, 10 Koret Way, #K113, San Francisco, CA 94143-0730, USA.
E-mail address: jacque.duncan@ucsf.edu (J.L. Duncan).

http://dx.doi.org/10.1016/j.ajoc.2017.04.001

amenable to recovery or response to experimental therapies despite not being visible on confocal AOSLO or SD-OCT images.

1. Introduction

Advances in ophthalmic imaging technology, such as spectral-domain optical coherence tomography (SD-OCT) and confocal adaptive optics scanning laser ophthalmoscopy (AOSLO), allow for detailed and sensitive measures of structural changes in the retina, including photoreceptors.[1,2] However, the relationship between images of cone structure and visual function is not always clear. This ambiguous relationship has been reported in acute macular neuroretinopathy (AMN), a disease characterized by selective injury to the cone photoreceptors with retention of the normal rod photoreceptor mosaic.[3] In follow-up of patients with AMN, persistent damage to the cone photoreceptor mosaic was documented at least one year after diagnosis, but some patients reported return of visual function despite documented abnormalities of cone structure.[4,5] Similar reports of function within areas of structural damage have been documented with other maculopathies, including macular telangiectasia type 2[6].

The objective of our study is to characterize foveal function in areas of apparent structural damage, which may provide insight into the relationship between structure and function given current technological advances in imaging.

2. Materials and methods

A patient presented after a viral illness with bilateral vision loss, mild vitritis, and SD-OCT and AOSLO images suggestive of focal cone loss at the fovea, findings diagnosed clinically as acute, bilateral foveolitis.

Informed consent was obtained after the study protocol and its associated risks were reviewed with the subject. The informed consent forms and study protocol were approved by the University of California San Francisco and University of California Berkeley Institutional Review Boards. The patient consented to publication of the findings of this study in writing. The patient was imaged 1 and 5 years after the initial diagnosis, but fundus-referenced tests of visual function were measured only at 5 years after symptom onset. The eye with better vision was chosen as the study eye based on visual acuity, fixation stability and AOSLO image quality.

2.1. Structural imaging

Complete eye examination including best-corrected visual acuity, color fundus photographs (Topcon 50EX, fundus camera, Topcon Medical Systems, Oakland, NJ), and infrared reflectance images (Spectralis HRA + OCT system [Heidelberg Engineering, Vista, CA, USA]) were completed after the study eye was dilated with one drop each of 1% tropicamide and 2.5% phenylephrine. SD-OCT b-scan images were obtained at 1° intervals through the central 20°, including the foveal avascular zone, at each visit. Horizontal SD-OCT scans through the PRL were exported to data analysis software (Igor Pro; WaveMetrics, Inc., Portland, OR) and manually segmented using sub-routines[7–11] to identify boundaries between the different retinal layers. Thickness of the outer nuclear layer at the fovea at visits 1 and 5 years after symptom onset was compared to measures from 20 normal subjects (mean age 45, standard deviation 10.2). Fundus-guided microperimetry (Nidek MP1, Nidek, Fremont, CA, USA) was measured in each eye 1 year after symptom onset in a light adapted state using a Goldmann III stimulus for 200 msec and 4–2 threshold strategy. The patient was asked to look in the center of 4 crosses, each 2° in size, located at 20° eccentricity around fixation.

Directional-OCT (D-OCT) was performed using an SD-OCT system with eye tracking on loan from Carl Zeiss Meditec (prototype). D-OCT is a technique whereby OCT images of the same structure are taken with three different illumination angles and analyzed using an approach that reveals the presence of structures in the retina with directional reflective properties. The full technique is described in other papers.[12,13] The purpose of the D-OCT measurements in this study was to look at the directionally-reflective properties of the waveguiding cone photoreceptors[14] and to explore the possibility of the presence of misdirected cones in the lesion of the patient.

A custom-built AOSLO system was used to obtain high-resolution images of the study eye as previously described.[15–17] AOSLO videos covering 1.2° × 1.2° of retina were processed to produce stabilized images that were assembled into montages which included the anatomic fovea, the macular area with IS/OS junction band disruption, and surrounding normal cones in the subject's eye.

2.2. Functional testing

Fundus-referenced visual testing was performed, including identification of the preferred retinal locus (PRL), an AOSLO-administered letter discrimination task, and fundus-guided microperimetry using a tracking SLO (TSLO). The method of identifying the PRL is described in a previous paper.[18] Areas identified by the SD-OCT images and AOSLO montages that suggested photoreceptor loss were specifically tested with the AOSLO discrimination task and with TSLO microperimetry.

2.2.1. AOSLO discrimination

An AOSLO-corrected discrimination task was performed to test visual function in and around the lesion. The test was a four-alternative-forced-choice tumbling 'E' task, where the letter E was directly projected onto the retina by modulating the 840 nm source in the AOSLO raster scan.[19] To the subject, the letter appeared as black on a dim (~4 cd/m^2) red background. The letter size was greater than the minimum threshold measured clinically (Snellen equivalent of 20/30) and was presented 125 times for a duration of one second on each trial (30 video frames). An AOSLO video was recorded for each trial, along with the subject responses. Since the stimulus was delivered by modulating the imaging beam, the stimulus was encoded directly into the video. As such, the exact location of the stimulus over the course of each 1-second trial was recorded. The analysis of the results was focused on those trials that remained within the lesion for the entire 1-second duration.

2.2.2. Fundus-guided microperimetry

The TSLO is a custom-built system that was modified to perform similar fundus-guided microperimetry testing as has been described for the AOSLO.[6,20] In both systems, accurate fundus-guided microperimetry is achieved via real-time, high-speed,

image-based eye-tracking.[21] The user interface allows the operator to identify and select specific regions in the retinal image to target for sensitivity threshold testing. The TSLO is a simple alternative to AOSLO in that it does not use adaptive optics to correct for ocular imperfections.

The main benefit of the TSLO over AOSLO microperimetry is that it offers more robust tracking performance over a larger field of view. The negative consequence of using TSLO for microperimetry is that transverse chromatic aberration is not objectively measured and corrected and the tracking performance and image quality is slightly worse. In this particular patient the TSLO was preferred over the AOSLO due to fixation instability which led to frequent AOSLO tracking failures. In the TSLO system, 840 nm light (Broadlighter, SuperLum, Cork, Ireland) was used to image the retina and 532 nm (CrystaLaser, Reno, NV, USA) was used for visible stimulation and threshold testing. This stimulation wavelength was chosen because it was convenient (readily available Diode Pumped Solid State laser) and because it excites L and M cones similarly with a ratio of ~0.8:1.[22]

The chromatic aberration was corrected in the TSLO system by adjusting the vergence and lateral displacement between the 532 nm and 840 nm scanning rasters until they both appeared equally sharp (longitudinal) and aligned (transverse) for the patient. The green background of approximately 100 cd/m^2 from the stimulus channel was sufficiently bright to remove any contribution from rod photoreceptors.[23]

The stimulus diameter was 4.5 arcminutes, roughly 70% that of a Goldmann I-sized stimulus. The stimulus was delivered for a duration of 200 ms (6 video frames) per trial to the target test site. An increment threshold approach was used to measure visual sensitivity; arbitrary units (au) were used to represent stimulus intensity on a linearized scale from 0 to 1 (a value of 0 represents background only; 1 corresponds to the strongest light deliverable by the system). The maximum luminance of our stimulus was 6532 cd/m^2, 1.82 log units higher than the background. The TSLO microperimetry results were generated using a 20-trial adaptive staircase guided by a yes-no response paradigm.[24] The threshold was measured three times at each retinal test site. Among the 9 test sites, 5 were targeted to fall within the lesion, and 4 outside the lesion in normal appearing retina as the control for this patient. A series of thresholds were recorded and averaged to create a single average value for each test site.

2.3. Image overlays

Retinal vascular landmarks and features were used to create image overlays combining color fundus photos, infrared fundus photos, and AOSLO images (Adobe Illustrator; Adobe Systems, Inc., San Jose, CA, USA). SD-OCT cross-sectional retinal images and lines representing the location of each scan were registered to the color fundus photo and AOSLO images.

3. Results

The patient presented with reduced visual acuity in the right eye to 20/80 with a yellow spot at the fovea on fundus examination (Fig. 1A), which subsequently evolved into a discrete hypopigmented lesion over 3 months with disruption of the IS/OS and OS/RPE junction bands (Fig. 1B). Fundus-guided microperimetry at 1 year after presentation revealed stable fixation (82% within 2°, 100% within 4 degrees of the center of 4 targets) with reduced sensitivity in the central 2°, but preserved function from 2 to 4°. Imaging at 1 (Fig. 1C) and 5 (Fig. 1D) years after disease onset showed no change in the appearance of the foveal lesion compared to 3 months after presentation, with color fundus photography showing a discrete circular lesion and SD-OCT scans obtained at 1° vertical intervals through the foveal avascular zone showing a disrupted IS/OS junction band with an intact ELM (Fig. 1). The outer nuclear layer thickness at the fovea measured 1 and 5 years after symptom onset (48.8 and 48.9 μm, respectively) were both reduced by more than 2 standard deviations below normal (mean 108.7, standard deviation 13.1 μm). Despite stability in the appearance of the lesion, visual acuity improved from the initial presentation of 20/80 (measured at 3 weeks and again at 1 year after initial symptom onset) to 20/25 5 years after symptom onset.

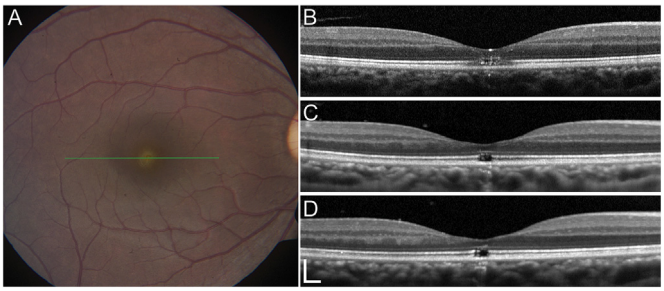

Fig. 1. Color fundus photography and spectral domain optical coherence tomography (SD-OCT) images. (A) Color fundus photo of the right eye at the time of presentation shows a yellow foveal lesion. The green line indicates the exact location of the SDOCT B-scan (Panel B) taken at that time. (B) The SD-OCT B-scan shows that the inner segment/outer segment (IS/OS) junction is disrupted in this and other scans obtained through the foveal avascular zone (FAZ). (C) The SD-OCT B-scan taken one year after presentation shows a clear break in the IS/OS junction across the lesion. (D) SD-OCT B-scan taken 5 years after presentation shows a disrupted IS/OS junction band with an intact overlying external limiting membrane without significant change compared to 1 year after presentation. Actual B-scan locations from panels C and D are very close but not exactly aligned with the B-scan in panel B. The scale bar, indicating 200 microns in the vertical and horizontal directions is in the lower left part of panel D and applies to all SD-OCT images. (For interpretation of the references to colour in this figure legend, the reader is referred to the web version of this article.)

Directional OCT analysis (Fig. 2) indicated that the focal region with diminished cone reflectivity could not be attributed to misdirected cones.

3.1. Structural images

Confocal AOSLO images showed reduced cone reflectivity at the area of the lesion identified by SD-OCT images and color fundus photography (Fig. 3). The cone mosaic within the lesion was discontinuous and RPE cell profiles were seen within the lesion, while cone mosaics appeared normal outside the discrete lesion, and cone spacing measures were within 1 standard deviation of age-similar normal mean values. SD-OCT images revealed discrete loss of the IS/OS junction or ellipsoid zone (EZ) band in the same region, and the external limiting membrane (ELM) band was irregular and hyper-reflective compared to the surrounding retina (arrowheads, Fig. 3). Both SD-OCT (foveal pit) and AOSLO images (radial symmetry of cone spacing) indicated that the lesion was centered on the anatomical fovea.

3.2. Functional testing

3.2.1. Preferred retinal locus

The PRL was identified to be within the lesion, or at the anatomical foveal location (white arrow, Fig. 4).

3.2.2. AOSLO-discrimination

We were able to trace the trajectory of the stimulus in 99 out of the 125 trials. The patient correctly identified the orientation of the tumbling E presented with AOSLO acuity testing to trials both

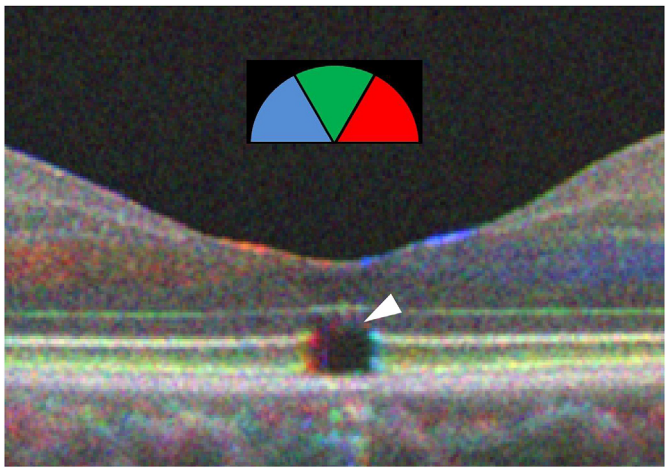

Fig. 2. Directional optical coherence tomography tricolor composite image. Regions of the spectral-domain optical coherence tomography image that are grayscale indicate structures that scatter equally when imaged from each direction. Blue, red and green structures are those that preferentially scatter when light is incident from the left, center and right directions, respectively. If misdirected cones were present, the inner segment/outer segment junction would have appeared within the lesion, but with a blue or red color indicating the pointing direction. Although there are some weak directional reflections originating within the lesion, there is no evidence of misdirected cones. Immediately posterior to the external limiting membrane centrally there is color (white arrowhead), indicating some directionally reflective structures in a location normally seen in grayscale. (For interpretation of the references to colour in this figure legend, the reader is referred to the web version of this article.)

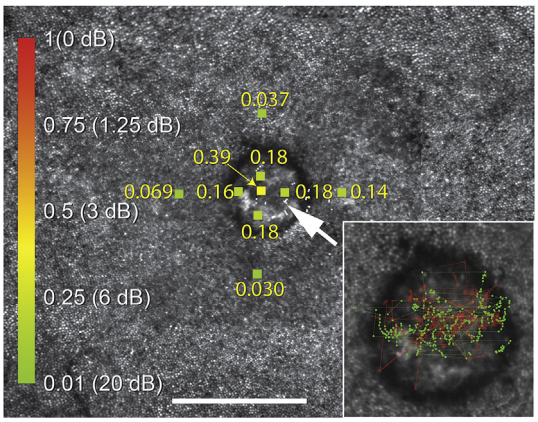

Fig. 4. Results of functional testing with preferred retinal locus (PRL), tracking scanning laser ophthalmoscope (TSLO) microperimetry, and adaptive optics SLO (AOSLO) acuity. The white arrowhead highlights the white dots within the lesion that identify the PRL. Most of the trials identifying the PRL fall within the lesion. The vertical bar uses colors to indicate threshold of perceived stimuli on a linear scale: green represents dimmest stimuli while red represents brightest stimuli. The scale bars indicate linear as well as dB units, which are computed from linear thresholds using the following equation: $10 \times \log_{10}(1/\text{threshold})$. Exact tested locations and stimulus size are indicated by the square boxes on the figure, and each is accompanied by text with the actual linear threshold values. TSLO microperimetry showed measurable but increased visual thresholds within the lesion. The inset shows results of the AOSLO acuity testing. Green trajectories (filled circles, solid line) indicate correct trials, whereas red trajectories (open circles, dashed line) indicate incorrect trials. Despite trajectories showing that the stimulus fell completely within the lesion for the duration of the trial, the patient was able to correctly identify the direction of the tumbling E in 48% of trials. Scale bar, 1°. (For interpretation of the references to colour in this figure legend, the reader is referred to the web version of this article.)

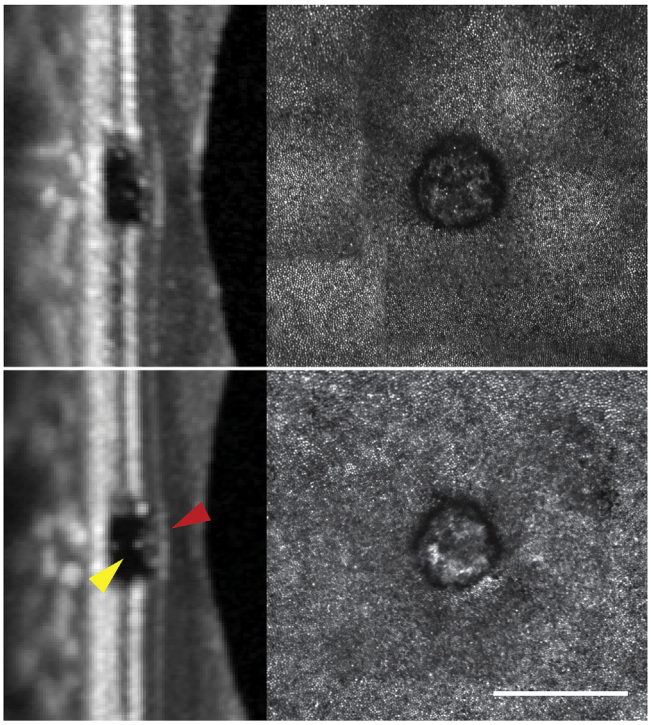

Fig. 3. Adaptive optics scanning laser ophthalmoscope and magnified spectral domain optical coherence tomography vertical B-scan images at 1 (top) and 5 (bottom) years after presentation. The red arrowhead indicates an intact but irregular and hyperreflective external limiting membrane compared to the surrounding retina. The yellow arrowhead indicates the discrete loss of the inner segment/outer segment junction band. Scale bar, 1°. (For interpretation of the references to colour in this figure legend, the reader is referred to the web version of this article.)

within and outside of the lesion. When the trajectory of the 'E' fell completely within the lesion for the duration of the trial (31 trials), the patient correctly identified its orientation 48% of the time (inset, Fig. 4). There is a 0.13% percent probability that this number of correct responses could happen by chance (Monte Carlo simulation of 20,000 trials). When the trajectory of the 'E' fell outside of the lesion for some of or all of the 1-second trial (68 trials), the patient correctly identified its orientation 78% of the time.

3.2.3. TSLO-microperimetry

TSLO microperimetry thresholds at all 9 sites tested showed measureable visual sensitivity (Fig. 4). Visual thresholds were increased more than 5-fold at the center of the lesion and more than 2.5-fold at the margins of the lesion compared to normal-appearing retina outside of the lesion.

4. Discussion

This is the first report of function within areas of apparent cone loss in long-term follow-up of a patient with acute bilateral foveolitis. Our report demonstrates measurable function in regions without a visible IS/OS junction band on OCT or cone profiles on confocal AOSLO imaging. This structural phenotype is not specific to this case; it has been observed in patients after retinal surgery[25] and with other maculopathies, such as cone-rod dystrophy, following blunt trauma, and macular telangiectasia.[6,26] The associated functional phenotype has only been shown in two cases of macular telangiectasia that we reported previously.[6] We cannot conclude that this phenotype is always associated with residual function, since the other reports did not test function in these regions. One exception is a report by Makous et al.,[27] albeit with a less similar phenotype. In that paper, function was tested in a patient with a mutation that gave rise to color blindness and AO images

with a cone mosaic interspersed with cone-sized non-reflecting regions (i.e., holes in the mosaic). Their functional testing suggested that these dark regions were absolute scotomas.

4.1. How can there be function in regions with no visible cells?

Importantly, the fact that a cell is not seen in SD-OCT or in confocal AOSLO should not be considered to offer conclusive evidence that no cell is present. Conversely, the measurement of function in a region *MUST* indicate that a cell is present, and that it is light-sensitive. The demonstration of spatial acuity (better-than-chance performance on a tumbling' 'E' task) within the lesion dispels any notion that the light sensitivity can be caused by light scattering into cones outside of the lesion.

Evidence of the presence of cells in regions exhibiting similar phenotypes to our patient (i.e. disrupted IS/OS junction bands, intact ELM on SD-OCT and little or no reflection from cones in confocal AOSLO), but with different conditions, is found in Scoles et al. where mosaics of cells are visible in the same regions using split-detection AOSLO.[26] Although they did not evaluate visual function in the same regions in their study, it was hypothesized that these cells were cone photoreceptor inner segments. The fact that we find visual function within similar regions not only supports the hypothesis that there are inner segments, but it also indicates that these cells contain excitable photopigment. Where this photopigment resides within the photoreceptor cell remains to be determined. In any case, the cells appear to lack the physical structures that give rise to the reflections that are normally seen in SD-OCT or confocal AOSLO images, but do not lack function. It is possible that the cone inner and outer segments are contracted up into the ELM, which may account for the slight hyper-reflectance seen at the ELM on SD-OCT images. Split detector images in regions that lack visible cones in confocal AOSLO images show cells that appear larger, and more irregular than a typical array of inner segments,[26] which may result in increased reflectivity in the ELM in SD-OCT images.

4.2. What is the prognosis for recovery?

In a previous report by our group on patients with macular telangiectasia that exhibit a similar phenotype, we showed that cones that did not appear in one visit regained fully reflective properties and exhibited normal function in a subsequent visit.[6] Studies on recovery after macular hole repair showed that following surgery, patients who had residual integrity of the ELM layer in OCT images had better visual outcomes compared to patients with disruptions in both the ELM and IS/OS junction band; the authors hypothesized that the ELM layer is critical for the restoration of the photoreceptor layer and for improvement of visual outcomes.[25]

The observation of functional cones in regions in which the ELM is intact despite disruption of the IS/OS junction band likely indicates the presence of cones that are amenable to recovery or treatment. These "dysflective" cones with abnormal reflective properties may be invisible on SD-OCT and AOSLO but, because they retain visual function, their presence is important for prognosis.

While evidence of a phenotype that may be common to many retinal diseases is mounting, a full analysis of structure and function in this phenotype that includes SD-OCT, confocal and split-detector AOSLO and accurate fundus-guided functional testing remains to be done in a single setting. This paper makes a strong case that such studies should be done.

5. Conclusions

The structural SD-OCT and AOSLO findings along with precise fundus-guided functional testing demonstrate that in lesions with a preserved ELM and disrupted IS/OS junction band, there may be cones with abnormal scattering characteristics that are not directly visible but retain some function. Although sensitivity thresholds in these abnormally scattering cones are elevated on functional testing, they still have measurable light sensitivity. After 5 years with a stable lesion indicating focal diminished cone reflectivity on SD-OCT and AOSLO scans, this case demonstrates that functional testing may indicate the presence of cones that may be amenable to recovery or treatment despite not being directly visible.

Acknowledgments and disclosures

Funding

All of the sources of funding for the work described in this publication are acknowledged below. The funding sources listed below had no role in the study design, data analysis or result interpretation. NIH Grants R01EY023591, EY002162, T32EY007043, K23 EY022412, K12EY017269, The Foundation Fighting Blindness (C-CL-0711-0530-UCSF01), Research to Prevent Blindness (to the Departments of Ophthalmology at UCLA and UCSF), The Giannini Foundation, The Lawrence L. Hillblom Foundation (2014-A-003-NET), The Beckman Initiative for Macular Research (#1201), The Macular Vision Research Foundation, The American Optometric Foundation, Hope For Vision, That Man May See, Inc., and the Harold and Pauline Price Foundation.

Conflict of interest

Austin Roorda has two patents on technology related to the Adaptive Optics Scanning Laser Ophthalmoscope. (USPTO #7,118,216 #6,890,076) These patents are assigned to both the University of Rochester and the University of Houston. The patents are currently licensed to Canon, Inc., Japan. Both Roorda and the company may benefit financially from the publication of this research. Brandon J. Lujan and Austin Roorda are inventors on a patent related to Directional Optical Coherence Tomography (USPTO patent #9,427,147). The patent is assigned to the University of California, Berkeley.

The following authors have no financial disclosures: JHT, KGF, KR, JQ, MBG, ETC, WT, JLD.

Authorship

All authors attest that they meet the current ICMJE criteria for Authorship.

Acknowledgements

The authors wish to acknowledge Lawrence Sincich for assistance with the manuscript.

References

1. Roorda A, Duncan JL. Adaptive optics ophthalmoscopy. *Annu Rev Vis Sci*. 2015;1:19–50.
2. Morgan JI. The fundus photo has met its match: optical coherence tomography and adaptive optics ophthalmoscopy are here to stay. *Ophthalmic Physiol Opt*. 2016;36:218–239.
3. Hansen SO, Cooper RF, Dubra A, Carroll J, Weinberg DV. Selective cone photoreceptor injury in acute macular neuroretinopathy. *Retina*. 2013;33:1650–1658.

4. Audo I, Gocho K, Rossant F, et al. Functional and high-resolution retinal imaging monitoring photoreceptor damage in acute macular neuroretinopathy. *Graefes Arch Clin Exp Ophthalmol*. 2016;254:855–864.
5. Mrejen S, Pang CE, Sarraf D, et al. Adaptive optics imaging of cone mosaic abnormalities in acute macular neuroretinopathy. *Ophthalmic Surg Lasers Imaging Retina*. 2014;45:562–569.
6. Wang Q, Tuten WS, Lujan BJ, et al. Adaptive optics microperimetry and OCT images show preserved function and recovery of cone visibility in macular telangiectasia type 2 retinal lesions. *Invest Ophthalmol Vis Sci*. 2015;56:778–786.
7. Birch DG, Wen Y, Locke K, Hood DC. Rod sensitivity, cone sensitivity, and photoreceptor layer thickness in retinal degenerative diseases. *Invest Ophthalmol Vis Sci*. 2011;52:7141–7147.
8. Hood DC, Lin CE, Lazow MA, Locke KG, Zhang X, Birch DG. Thickness of receptor and post-receptor retinal layers in patients with retinitis pigmentosa measured with frequency-domain optical coherence tomography. *Invest Ophthalmol Vis Sci*. 2009;50:2328–2336.
9. Hood DC, Ramachandran R, Holopigian K, Lazow M, Birch DG, Greenstein VC. Method for deriving visual field boundaries from OCT scans of patients with retinitis pigmentosa. *Biomed Opt Express*. 2011;2:1106–1114.
10. Wen Y, Klein M, Hood DC, Birch DG. Relationships among multifocal electroretinogram amplitude, visual field sensitivity, and SD-OCT receptor layer thicknesses in patients with retinitis pigmentosa. *Invest Ophthalmol Vis Sci*. 2012;53:833–840.
11. Wen Y, Locke KG, Klein M, et al. Phenotypic characterization of 3 families with autosomal dominant retinitis pigmentosa due to mutations in KLHL7. *Arch Ophthalmol*. 2011;129:1475–1482.
12. Lujan BJ, Roorda A, Croskrey JA, et al. Directional optical coherence tomography provides accurate outer nuclear layer and Henle fiber layer measurements. *Retina*. 2015;35:1511–1520.
13. Lujan BJ, Roorda A, Knighton RW, Carroll J. Revealing Henle's fiber layer using spectral domain optical coherence tomography. *Invest Ophthalmol Vis Sci*. 2011;52:1486–1492.
14. Gao W, Cense B, Zhang Y, Jonnal RS, Miller DT. Measuring retinal contributions to the optical Stiles-Crawford effect with optical coherence tomography. *Opt Express*. 2008;16:6486–6501.
15. Duncan JL, Zhang Y, Gandhi J, et al. High-resolution imaging with adaptive optics in patients with inherited retinal degeneration. *Invest Ophthalmol Vis Sci*. 2007;48:3283–3291.
16. Merino D, Duncan JL, Tiruveedhula P, Roorda A. Observation of cone and rod photoreceptors in normal subjects and patients using a new generation adaptive optics scanning laser ophthalmoscope. *Biomed Opt Express*. 2011;2:2189–2201.
17. Talcott KE, Ratnam K, Sundquist SM, et al. Longitudinal study of cone photoreceptors during retinal degeneration and in response to ciliary neurotrophic factor treatment. *Invest Ophthalmol Vis Sci*. 2011;52:2219–2226.
18. Ratnam K, Carroll J, Porco TC, Duncan JL, Roorda A. Relationship between foveal cone structure and clinical measures of visual function in patients with inherited retinal degenerations. *Invest Ophthalmol Vis Sci*. 2013;54:5836–5847.
19. Poonja S, Patel S, Henry L, Roorda A. Dynamic visual stimulus presentation in an adaptive optics scanning laser ophthalmoscope. *J Refract Surg*. 2005;21:S575–S580.
20. Tuten WS, Tiruveedhula P, Roorda A. Adaptive optics scanning laser ophthalmoscope-based microperimetry. *Optometry Vis Sci*. 2012;89:563–574.
21. Arathorn DW, Yang Q, Vogel CR, Zhang Y, Tiruveedhula P, Roorda A. Retinally stabilized cone-targeted stimulus delivery. *Opt Express*. 2007;15:13731–13744.
22. Schnapf JL, Kraft TW, Baylor DA. Spectral sensitivity of human cone photoreceptors. *Nature*. 1987;325:439–441.
23. Aguilar M, Stiles WS. Saturation of the rod mechanism of the retina at high levels of stimulation. *J Mod Opt*. 1954;1:59–65.
24. Watson AB, Pelli DG. QUEST: a Bayesian adaptive psychometric method. *Percept Psychophys*. 1983;33:113–120.
25. Landa G, Gentile RC, Garcia PM, Muldoon TO, Rosen RB. External limiting membrane and visual outcome in macular hole repair: spectral domain OCT analysis. *Eye (Lond)*. 2012;26:61–69.
26. Scoles D, Flatter JA, Cooper RF, et al. Assessing photoreceptor structure associated with ellipsoid zone disruptions visualized with optical coherence tomography. *Retina*. 2016;36:91–103.
27. Makous W, Carroll J, Wolfing JI, Lin J, Christie N, Williams DR. Retinal microscotomas revealed with adaptive-optics microflashes. *Invest Ophthalmol Vis Sci*. 2006;47:4160–4167.